Available online at www.sciencedirect.com

ScienceDirect

Mendeleev Commun., 2022, **32**, 317–319

Mendeleev Communications

Solvothermal modification of graphitic C_3N_4 with Ni and Co phthalocyanines: structural, optoelectronic and surface properties

Lev A. Lebedev,* Maria I. Chebanenko, Ekaterina V. Dzhevaga, Kirill D. Martinson and Vadim I. Popkov

Ioffe Institute, Russian Academy of Sciences, 194021 St. Petersburg, Russian Federation.
E-mail: l.a.lebedev@mail.ioffe.ru

DOI: 10.1016/j.mencom.2022.05.008

Nanocomposites for photocatalytic applications were obtained by alchothermal modification of g-C_3N_4 with cobalt(II) and nickel(II) phthalocyanine complexes. The nanocomposites demonstrated higher photocatalytic activity than the bare matrix and stability under actinic irradiation. In the optoelectronic structure of the composites, the E_g value of the g-C_3N_4 matrix increased to 3.05 eV, while for MPc agents, it decreased from 1.96 to 1.82 eV.

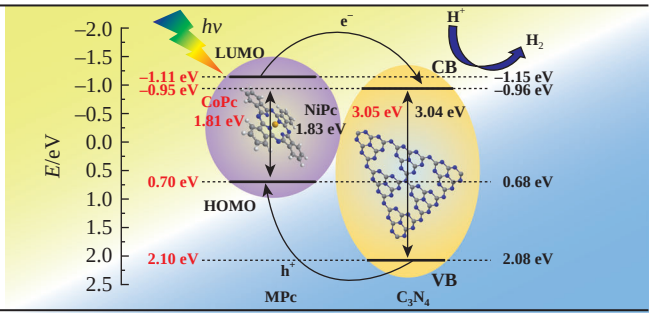

Keywords: doped carbon materials, graphitic carbon nitride, phthalocyanines, solvothermal synthesis, photocatalysts.

Photocatalytic materials have become more attractive due to their capabilities in the last few decades. A wide variety of materials have been successfully used in photocatalytic systems, and among them, chalcogenides, mainly oxides, are the most common inorganic materials due to their high stability. Titania,[1–4] zirconia,[5] zinc oxide[6] and ceria[7] find their application in hydrogen reforming, photovoltaic systems and others. Several photoactive organic aromatic chlorophyll-like compounds are used in photoactive systems.[8] In order to obtain materials suitable for UV-VIS applications, chemists have used several methods to extend the operating wavelength ranges, such as photosensitization with organic dyes,[9] the use of multi semiconductor systems[3,10] and doping with noble metal nanoparticles.[1,11–13] Another aspect of efficient heterogeneous catalysis is the working surface. Easily produced non-metallic material with superior operating wavelength (up to 460 nm) can be modified with graphitic carbon nitride (g-C_3N_4) to increase surface area.[14–17]

In this work, pure g-C_3N_4 was modified by alchothermal treatment with cobalt(II) and nickel(II) phthalocyanine (CoPc and NiPc) complexes to improve photocatalytic performance. Because metal phthalocyanines (MPc) are known for their thermal and chemical stability, visible light activity and high light absorbance, they are also used in organic semiconductor assemblies, photovoltaic systems and photosensitizers.[18,19] Alchothermal modification provides the g-C_3N_4/MPc nanocomposite with a uniform distribution of MPc.

Powder X-ray diffraction analysis shows the formation of MPc crystallites in the g-C_3N_4/MPc composite (Figure 1). Moreover, the phthalocyanine peaks appear to be sharp, occupying the same positions in the free form and composite structures. This result indicates a well-crystallized structure, and the carbon nitride peaks do not differ between the samples, which evidences the absence of any changes in its structure during alchothermal synthesis. The peaks of phthalocyanine derivatives are specific for the monoclinic β-modification (ICDD #00-011-0744) with space group $P2_1/c$.[20,21]

The infrared spectra of the nanocomposites (Figure S3, see Online Supplementary Materials) reveal an intense absorption band at 1634 cm^{-1}, corresponding to deformation vibrations of the

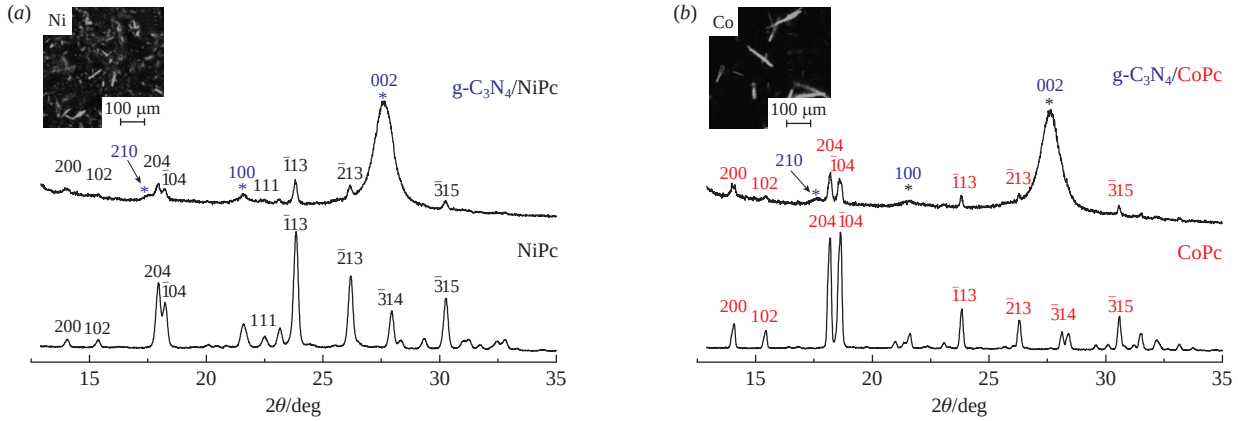

Figure 1 Powder X-ray diffraction patterns of (*a*) initial NiPc and g-C_3N_4/NiPc composite, as well as (*b*) initial CoPc and g-C_3N_4/CoPc composite; *hkl* values marked with * correspond to g-C_3N_4. Insets: SEM micrographs showing the distribution of MPc in composites.

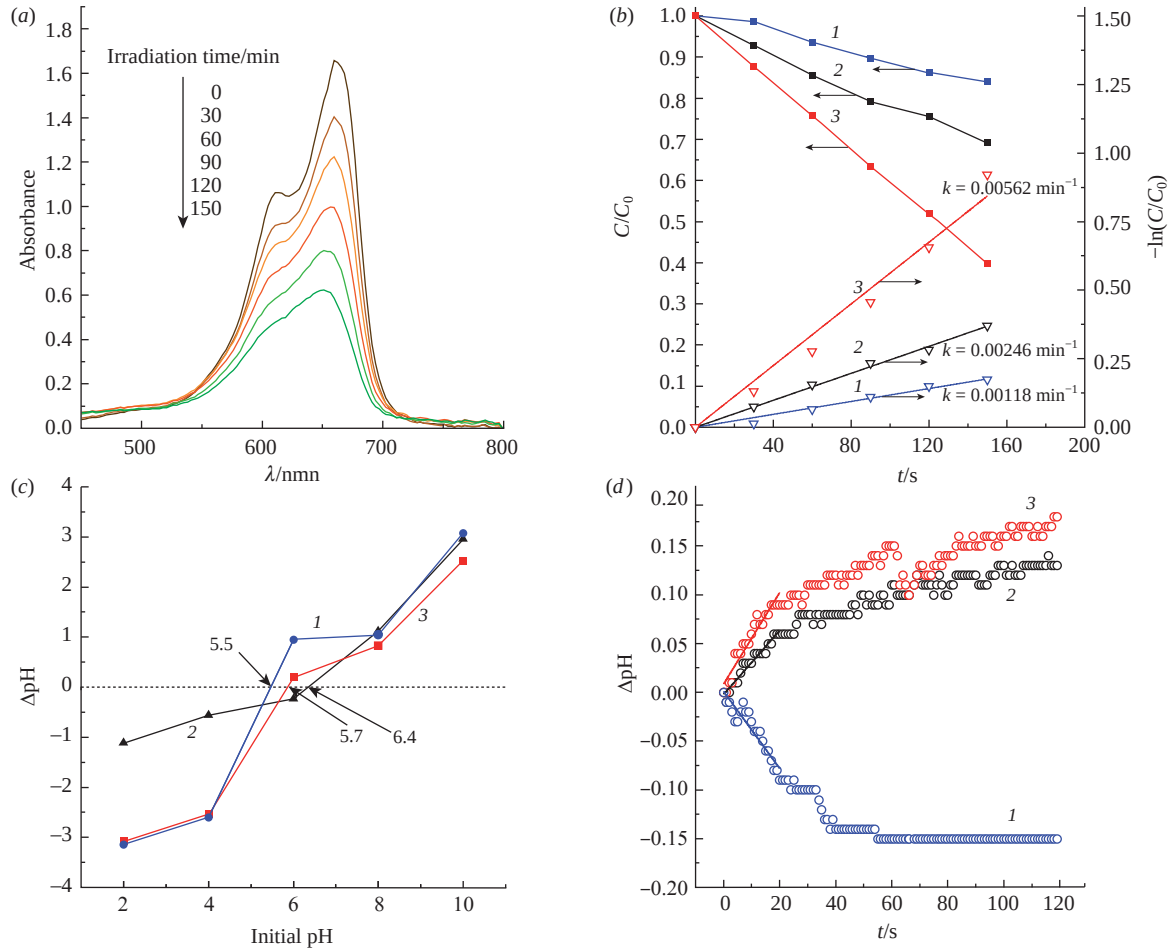

Figure 2 (*a*) Change in UV-VIS absorption upon photocatalytic MB decolorization with g-C_3N_4/CoPc catalyst, (*b*) MB concentration variation and photocatalytic MB decolorization kinetics using different photocatalysts, (*c*) point of zero charge curves and (*d*) pH kinetic curves for different photocatalysts. Photocatalysts used: (*1*) pure g-C_3N_4, (*2*) g-C_3N_4/NiPc and (*3*) g-C_3N_4/CoPc.

O–H bonds in physically adsorbed water molecules. Other bands can be attributed to g-C_3N_4 and metal phthalocyanine structures. However, due to the similarity of structures and the higher concentration of carbon nitride, some phthalocyanine peaks may be low in intensity or indistinguishable. The absorption band in the region of 1655 cm^{-1} is caused by bending vibrations of the N–H bonds. An intense absorption band at 816 cm^{-1} and low-intensity absorption bands with peaks at wavenumbers from 1572 to 1239 cm^{-1} are assigned to deformation and stretching vibrations of the C–N bonds of the heptazine ring of g-C_3N_4, respectively. The band at 1318 cm^{-1} is due to the vibrations of the C=N–C fragment at bridge sites, and the tiny peak at 1164 cm^{-1} is characteristic of the Ni–N bond in NiPc.[14,22]

SEM images and element mapping of g-C_3N_4/MPc samples are shown in Figures 1 (insets) and S1. The synthesized nanocomposite is agglomerated g-C_3N_4 particles consisting of smaller fragments with a large surface area. MPc is deposited on the surface of carbon nitride as needle-shaped crystals uniformly distributed over the surface of g-C_3N_4 particles. This crystal structure is characteristic of the monoclinic type β-NiPc, usually formed under solvothermal conditions. There is no significant change in the morphology of carbon nitride, but the formation of a heterojunction is possible upon contact with crystals of phthalocyanine derivatives. Low-temperature N_2 adsorption–desorption isotherms are shown in Figure S3. According to the IUPAC classification, these isotherms can be classified as type IV, which means that the CoPc and NiPc composites with g-C_3N_4 have a mesoporous structure. Both isotherms have hysteresis loops in the range of 0.85–1.0 relative values and are classified as H3. This fact points out the slit-shaped type of pores. An analysis of the differential curves of pore size distribution makes it possible to determine that the predominant pore sizes in the structure of nanocomposites are 10–30 and 30–85 nm. According to the insets, the mean pore sizes for g-C_3N_4/NiPc and g-C_3N_4/CoPc are 17.9 and 19.9 nm, respectively. The surface area values measured by the BET method are 78.4 and 66.8 $m^2\ g^{-1}$, which are somewhat lower than those of the initial g-C_3N_4 (81.8 $m^2\ g^{-1}$) used for the synthesis.[14,15] The decrease in surface area can be caused by several factors, such as carbon nitride agglomeration, pore plugging by phthalocyanine crystals or slight changes in morphology due to the solvothermal process.

The electronic structure of the nanocomposites was calculated from the DRS spectra using the Kubelka–Munk function shown in Figure S4(*b*). The calculated band gap values for phthalocyanines, graphitic carbon nitride and nanocomposites are shown in Table S1. It can be noticed that the band gap of free agents changed after the formation of the nanocomposite, leading, in particular, to an increase in the band gap of g-C_3N_4, which can also be associated with changes in surface groups due to alchothermal treatment. For MPc, this type of deviation may be related to the recrystallization process during synthesis or MPc–substrate interactions.[18,23–25] Nevertheless, a heterojunction is formed, so it can provide a wider operating spectrum due to phthalocyanine derivatives.

The photochemical activity was tested on a Fenton-like system by measuring methylene blue (MB) decolorization when exposed to 70 W Xe lamp light through a UV cutoff filter [Figure 2(*a*)]. As can be seen from Figure 2(*b*), composites have a higher efficiency than unmodified carbon nitride. The stability of the composite was

also measured under the same irradiation conditions: the composites did not show any significant changes after four hours of exposure to actinic light, all deviations were within tolerance.

The surface groups were characterized by the point of zero charge (PZC) method [Figure 2(*c*)] and the pH kinetic curve method[26] [Figure 2(*d*)]. From the PZC analysis, it was concluded that all materials have acidic surface groups, but the PZC values for composites are biased towards basic pH values. This trend can also be observed in the pH kinetic curves related to the integral acidity of the surface of a solid sample in contact with a solvent. The pristine g-C_3N_4 exhibits the behavior inherent in the presence of acidic groups, in contrast to both MPc composites, which exhibit exactly the opposite behavior (Table S2). The integral pH value of carbon nitride is in the acidic region if the synthesis process takes place in the air, which leads to oxidation of the edges of the g-C_3N_4 sheets and, presumably, to the formation of carboxyl groups. The donor-type MPc complex causes a change in surface behavior after modification with phthalocyanine. This type of donor–acceptor interaction in the nanocomposite makes it suitable for photocatalytic reforming and CO_2 reduction.

In summary, the g-C_3N_4/MPc (M = Ni and Co) nanocomposites were successfully obtained by alchothermal modification. It is shown that the applied modification technique leads to a uniform distribution of MPc crystals without significant changes in the surface area of the samples. At the same time, the g-C_3N_4/MPc heterojunction is formed, providing better absorption of visible light and, consequently, higher photocatalytic efficiency is expected. Moreover, surface modification alters the integral acidity, resulting in the formation of basic sites. Therefore, the modification of g-C_3N_4 provides a wider operating spectrum due to the absorption of phthalocyanine in the visible range, while the basic sites and heterojunction structure promote photocatalysis. This work proposes a simple alchothermal process for the production of g-C_3N_4/MPc nanocomposites for photocatalytic applications, as well as other phthalocyanine-sensitized materials.

This work was performed using the analytical equipment of the Engineering Center of the St. Petersburg State Institute of Technology.

Online Supplementary Materials

Supplementary data associated with this article can be found in the online version at doi: 10.1016/j.mencom.2022.05.008.

References

1 A. Yu. Kurenkova, A. M. Kremneva, A. A. Saraev, V. Murzin, E. A. Kozlova and V. V. Kaichev, *Catal. Lett.*, 2021, **151**, 748.
2 M. V. Korolenko, P. B. Fabritchnyi and M. I. Afanasov, *Mendeleev Commun.*, 2020, **30**, 770.
3 M. N. Lyulyukin, A. Y. Kurenkova, A. V. Bukhtiyarov and E. A. Kozlova, *Mendeleev Commun.*, 2020, **30**, 192.
4 A. A. Rempel, A. A. Valeeva, A. S. Vokhmintsev and I. A. Weinstein, *Russ. Chem. Rev.*, 2021, **90**, 1397.
5 M. Mansouri, N. Mozafari, B. Bayati and N. Setareshenas, *Bull. Mater. Sci.*, 2019, **42**, 230.
6 O. Długosz and M. Banach, *J. Nanostruct. Chem.*, 2021, **11**, 601.
7 Y. Li, J. Lin, B. Xie and G. Liu, *J. Wuhan Univ. Technol., Mater. Sci. Ed.*, 2020, **35**, 335.
8 E. M. Nasir, M. T. Hussein and A. H. Al-Aarajiy, *Adv. Mater. Phys. Chem.*, 2019, **9**, 158.
9 J. Xu, Y. Li, S. Peng, G. Lu and S. Li, *Phys. Chem. Chem. Phys.*, 2013, **15**, 7657.
10 S. M. Tikhanova, L. A. Lebedev, K. D. Martinson, M. I. Chebanenko, I. V. Buryanenko, V. G. Semenov, V. N. Nevedomskiy and V. I. Popkov, *New J. Chem.*, 2021, **45**, 1541.
11 A. V. Stavitskaya, E. A. Kozlova, A. Yu. Kurenkova, A. P. Glotov, D. S. Selischev, E. V. Ivanov, D. V. Kozlov, V. A. Vinokurov, R. F. Fakhrullin and Y. M. Lvov, *Chem. – Eur. J.*, 2020, **26**, 13085.
12 E. A. Kozlova, A. Yu. Kurenkova, E. Yu. Gerasimov, N. V. Gromov, T. B. Medvedeva, A. A. Saraev and V. V. Kaichev, *Mater. Lett.*, 2021, **283**, 128901.
13 D. Vasilchenko, P. Topchiyan, A. Tsygankova, T. Asanova, B. Kolesov, A. Bukhtiyarov, A. Kurenkova and E. Kozlova, *ACS Appl. Mater. Interfaces*, 2020, **12**, 48631.
14 M. I. Chebanenko, N. V. Zakharova, A. A. Lobinsky and V. I. Popkov, *Semiconductors*, 2019, **53**, 2072.
15 M. I. Chebanenko, N. V. Zakharova and V. I. Popkov, *Russ. J. Appl. Chem.*, 2020, **93**, 494 (*Zh. Prikl. Khim.*, 2020, **93**, 490).
16 M. Chebanenko, A. A. Lobinsky and V. I. Popkov, *15th International Meeting 'Fundamental Problems of Solid State Ionics'*, Chernogolovka, Russia, 2020, p. 442.
17 M. I. Chebanenko, K. D. Martinson, I. V. Matsukevich and V. I. Popkov, *Nanosyst.: Phys., Chem., Math.*, 2020, **11**, 474.
18 A. M. Sevim, *J. Organomet. Chem.*, 2017, **832**, 18.
19 M. Lu, Z. Sun, Y. Zhang, Q. Liang, M. Zhou, S. Xu and Z. Li, *Synth. Met.*, 2020, **268**, 116480.
20 M. M. El-Nahass, K. F. Abd-El-Rahman, A. A. M. Farag and A. A. A. Darwish, *Phys. Scr.*, 2006, **73**, 40.
21 P. Ballirano, R. Caminiti, C. Ercolani, A. Maras and M. A. Orrù, *J. Am. Chem. Soc.*, 1998, **120**, 12798.
22 F. Sánchez-De la Torre, J. Rivera De la Rosa, B. I. Kharisov and C. J. Lucio-Ortiz, *Materials*, 2013, **6**, 4324.
23 K. J. Hamam and M. I. Alomari, *Appl. Nanosci.*, 2017, **7**, 261.
24 N. R. Armstrong, D. Alloway, A. Graham, C. Shallcross, M. Brumbach, P. A. Veneman, D. Placencia and W. Wang, *Proc. SPIE 7034, Physical Chemistry of Interfaces and Nanomaterials VII*, 2008, 703402.
25 B. Joseph and C. S. Menon, *E-J. Chem.*, 2007, **4**, 255.
26 E. A. Pakhnutova and Yu. G. Slizhov, *Russ. J. Phys. Chem. A*, 2014, **88**, 1408 (*Zh. Fiz. Khim.*, 2014, **88**, 1228).

Received: 14th October 2021; Com. 21/6720